Searching for Idealized Prototype Learning for Interpreting Multi-Layered Neural Networks

Ryotaro Kamimura
Tokai University, Kitanakame, Hiratsuka, Kanagawa, 259-1292, Kanagawa, Japan

Keywords: Prototype Learning, Non-Prototype Learning, Activation Function, Potentiality, Ratio Potentiality, Entropy, Divergence, Interpretation.

Abstract: The present paper aims to show that neural learning consists of two fundamental phases: prototype and non-prototype learning in an ideal state. The prototype refers to a network with the simplest configuration, ideally determined without the influence of inputs. However, in actual learning, prototype and non-prototype learning are mixed and entangled. To demonstrate the existence of these two phases in an ideal state, it is necessary to explicitly distinguish between networks that are exclusively focused on acquiring the prototype and those that target non-prototype properties. We use different activation functions, combined serially, to represent the prototype and non-prototype learning phases. By combining multiple different activation functions, it is possible to create networks that exhibit both prototype and non-prototype properties in an almost ideal state. This method was applied to a business dataset that required improved generalization as well as interpretation. The experimental results confirmed that the ReLU activation function could identify the prototype with difficulty, while the hyperbolic tangent function could more easily detect the prototype. By combining these two activation functions within one framework, generalization performance could be improved while maintaining representations that are as close as possible to those obtained during prototype learning, thus facilitating easier interpretation.

1 INTRODUCTION

1.1 Idealized Prototype Learning

The concept of prototype learning has received significant attention over the years (Saralajew et al., 2018). If an informative exemplar, or prototype, can be identified, learning in neural networks becomes much more efficient, enabling faster training and evaluation. This could address the problem of massive data requirements for training multi-layered neural networks. Furthermore, prototypes offer greater interpretability, which is crucial, given the black-box nature of neural networks, especially as these networks become larger and more complex.

As mentioned above, conventional methods have typically focused on prototypes as representative examples of input data sets. In contrast, the prototype discussed in this paper is intended to serve as the foundation for constructing basic neural networks, from which actual multi-layered neural networks can be derived. For instance, we can imagine a prototype that is self-organized, utilizing network resources as minimally as possible. This prototype should be extracted or constructed at the beginning of learning, followed by ordinary, non-prototype learning to achieve faithful representations of the inputs.

To explain the prototype more concretely in the context of neural networks as discussed in this paper, we assume that any multi-layered neural network can be generated from a corresponding prototype, hidden within the network. This prototype is a network without hidden layers, where all components, such as neurons and weights, are connected independently and separately. It is important to note that this prototype is not intended to faithfully represent the inputs but rather to represent the given network resources as minimally as possible.

However, the distinction between prototype and non-prototype learning is not always clear in actual learning processes. In practice, these two types of learning are often intertwined, making it difficult to distinguish between them. To address this, we first attempt to differentiate between networks dedicated to prototype learning and those focused on non-prototype learning. Subsequently, we aim to combine

Kamimura, R.
Searching for Idealized Prototype Learning for Interpreting Multi-Layered Neural Networks.
DOI: 10.5220/0013047600003837

In *Proceedings of the 16th International Joint Conference on Computational Intelligence (IJCCI 2024)*, pages 475-487
ISBN: 978-989-758-721-4; ISSN: 2184-3236

these networks within a single framework to achieve and examine the ideal learning process that incorporates both prototype and non-prototype learning.

Then, we need to identify a network where the prototype is easily recognizable and another where the prototype is not as easily identified. There are various ways to create different configurations, and in this context, we propose using multiple activation functions within a single framework to realize different properties. If our hypothesis of prototype and non-prototype learning holds true, one of the major challenges in selecting appropriate activation functions lies in the pursuit of finding the best possible function or an idealized activation function that works across all scenarios, including both prototype and non-prototype learning (Ramachandran et al., 2017). Given that the properties of these two phases are likely to be strongly interwoven, it may be impossible to find a single appropriate activation function for all situations.

In this paper, we attempt to generate networks with different properties to enhance interpretation and generalization by using different activation functions. We then combine these activation functions to produce an idealized prototype for network configuration. The primary objective of this paper is to examine how the combination of different activation functions can influence the performance of the corresponding network, based on the assumption that every learning process comprises both prototype learning and non-prototype learning.

1.2 Main Contributions

The main contributions of this paper can be summarized as follows.

- This paper shows that a prototype exists behind complex multi-layered neural networks. The prototype is assumed to be a network without hidden layers, with components that are independently and separately connected. Consequently, the learning process of neural networks should consist of both prototype and non-prototype learning. Prototype learning aims to identify the simplest possible network, while non-prototype learning focuses on processing detailed information in the inputs.
- Because pure prototype and non-prototype learning cannot be easily achieved, we attempt to produce networks that are relatively better at detecting the prototype, and others that are not as proficient at doing so. To create these different networks, we introduce a method to vary the activation function and attempt to incorporate multiple activation functions within one framework. We aim to demonstrate the effectiveness of this method in improving generalization while maintaining network configurations as close as possible to their simplest form. This can enhance interpretability, which is the main objective of prototype learning.

1.3 Paper Organization

In Section 2, we present some related studies on the activation function, few-shot learning, and U-shaped learning, emphasizing the differences between our method and conventional methods. In Section 3, we show multiple activation functions, combining the tangent and ReLU activation functions, corresponding to prototype and non-prototype learning. In particular, we explain why prototype and non-prototype learning correspond to the tangent and ReLU functions. Then, after briefly explaining the difference between prototype and non-prototype learning, the potentiality is introduced, based on the absolute values of connection weights. For comparing the prototype and compressed networks, we introduce the ratio potentiality of the compressed to the supposed prototype network. In Section 4, we present results using a simple business dataset. The results confirmed that the combination of tangent and ReLU functions could detect higher ratio potentiality in prototype learning and higher generalization in non-prototype learning.

2 RELATED WORK

We explain three main related works: activation functions, few-shot learning, and U-shaped learning briefly.

First, the activation function plays an important role in creating prototype learning. According to our hypothesis, prototype learning aims to extract the prototype for network configurations, while non-prototype learning focuses on processing detailed information from inputs and their relations to outputs. Therefore, it is natural that the activation function should change depending on the learning objective. There are numerous activation functions that address computational issues such as vanishing gradients, computational load, and sparsity (Ramachandran et al., 2017; Nwankpa et al., 2018; Jagtap and Karniadakis, 2023; Emanuel et al., 2024). Additionally, activation functions have become adaptive with parameters, and ensemble and combined activation functions have been found to perform well (Sütfeld et al., 2020; Apicella et al., 2021; Jagtap and Karni-

adakis, 2023).

Our method of idealized prototype learning is based on the combination of different activation functions. At present, the activation functions are fixed-type, but if trainable activation functions could be used (Sütfeld et al., 2020), the method might approach idealized prototype learning. However, one of the major differences is that, unlike most conventional methods aimed at improving generalization, our method seeks to interpret the inner workings of neural networks by positing the existence of a prototype, which should exist for all neural networks. The prototype is not obtained by training neural networks but is assumed to exist behind any multi-layered neural network.

Second, the prototype learning proposed here differs from conventional methods. Prototype learning has received considerable attention recently, as complex datasets require equally complex neural networks for learning. If many inputs are classified under one prototype, learning can be significantly easier (Kim et al., 2019; Song et al., 2023). Additionally, in so-called "zero-shot" learning (Chao et al., 2016; Pourpanah et al., 2022), the concept of a prototype becomes more abstract, eventually leading to no actual prototypes being used. Instead, semantic features are introduced to relate seen and unseen inputs. Although the concept becomes more abstract to improve generalization, these methods still focus on input properties. The prototype in this paper becomes increasingly abstract, minimizing or even excluding semantic information about inputs as much as possible. The prototype is not for coming inputs but is solely for the network configuration itself. Within the given network resources, neural networks attempt to self-organize as simply and economically as possible. Only after this prototype learning process should actual non-prototype learning begin. This suggests the possibility of extending the concept of a prototype to different areas.

Third, prototype learning can be viewed as an extended version of the well-known U-shaped learning. Prototype learning is strongly related to U-shaped learning, particularly in the context of language acquisition problems (Westermann, 2022). This problem was initially associated with the attempt to unify regular and irregular forms in natural language using neural networks or connectionist models (Rumelhart and McClelland, 1986; Pinker and Prince, 1988; Kirov and Cotterell, 2018; Corkery et al., 2019). Children initially use language rules correctly, then enter a period of overgeneralization, where irregular verbs are treated as regular ones. Eventually, they learn to use both regular and irregular forms correctly. U-shaped learning has been actively discussed not only in cognitive development but also in many other fields, particularly in computational learning (Carlucci and Case, 2013; Case and Kötzing, 2016; Viering and Loog, 2022).

In our framework, the phase of overgeneralization corresponds to the phase of prototype learning. Children do not initially try to extract abstract rules of language but rather explore the permissible conditions within given physical and mental constraints. Within these constraints, they then attempt to simplify and clarify these physical and mental components as much as possible. We can say that rule acquisition in language learning occurs during the phase of non-prototype learning, which corresponds to the final phase of learning. This may explain why U-shaped learning is observed in so many different fields.

3 THEORY AND COMPUTATIONAL METHODS

3.1 Prototype and Non-Prototype Learning

The idealized prototype learning is illustrated in Figure 1(a), where, at the beginning, a network attempts to acquire its prototype, which is the minimal possible network configuration. After completing this prototype learning, non-prototype learning begins, aiming to acquire as much detailed information about the inputs as possible. However, in actual situations, prototype learning is mixed or entangled with corresponding non-prototype learning, making it sometimes impossible to separate them, as shown in Figure 1(b). It is important to note that even in this entangled and mixed case, prototype learning is assumed to exist at the deepest level of learning. When it is almost impossible to extract the prototype, we attempt to train several networks independently to search for candidate networks for prototype or non-prototype learning, as depicted in Figure 1(c). Finally, these independently trained networks are serially arranged to estimate the ideal prototype learning, as shown in Figure 1(d).

3.2 Multiple Activation Functions

We use different activation functions for different learning schemes within one framework (Sütfeld et al., 2020). Let us compute the input u_{jk} to the neuron from the nth layer to the $n+1$th layer, labeled (n, n+1), using an idealized activation function. In an ideal state, it is assumed that two distinct activation

functions are used for the two types of learning:

$$v_{jk}^{(n,n+1)} = \alpha\,\mathrm{Proto}(u_{jk}^{(n,n+1)}) + (1-\alpha)\,\mathrm{NProto}(u_{jk}^{(n,n+1)}), \quad (1)$$

where "Proto" and "NProto" represent the activation functions for the prototype and non-prototype learning, respectively, and the parameter α is set to one for prototype learning and zero for non-prototype learning.

This idealized prototype learning cannot be easily realized because it is impossible to know which activation function is appropriate for the specific learning phase. Therefore, as shown in Figure 1(c), we independently train different networks with different activation functions, searching for the appropriate ones for the specific learning phase. For example, in the experiments below, it is experimentally shown that the hyperbolic tangent function can clearly extract the prototype, while the ReLU activation function cannot extract the prototype as effectively. However, this may be specific to our experiments. We then combine two conventional activation functions as follows:

$$v_{jk}^{(n,n+1)} = \alpha\,\mathrm{Tanh}(u_{jk}^{(n,n+1)}) + (1-\alpha)\,\mathrm{ReLU}(u_{jk}^{(n,n+1)}). \quad (2)$$

In the actual learning process, as shown in Figure 1(d), the hyperbolic tangent function is used at the beginning, followed by the ReLU activation function in subsequent steps. In the actual learning, for the first fixed number of learning steps, α is set to one, meaning the hyperbolic tangent function is used initially.

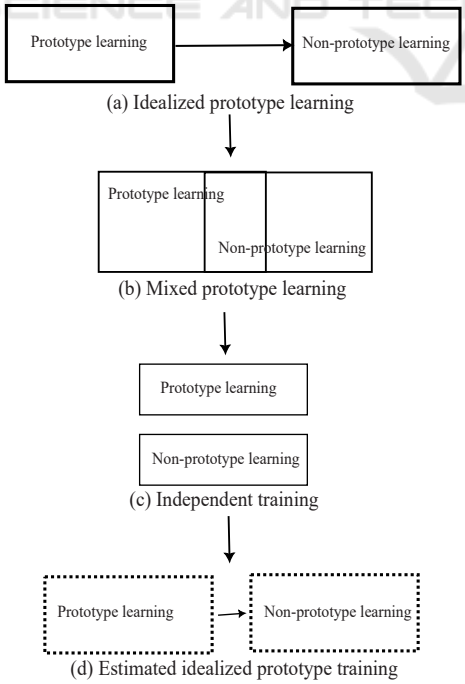

Figure 1: Concept of idealized prototype learning and its actualization learning.

Afterward, the parameter is set to zero, meaning the ReLU activation function is used for the remaining learning steps.

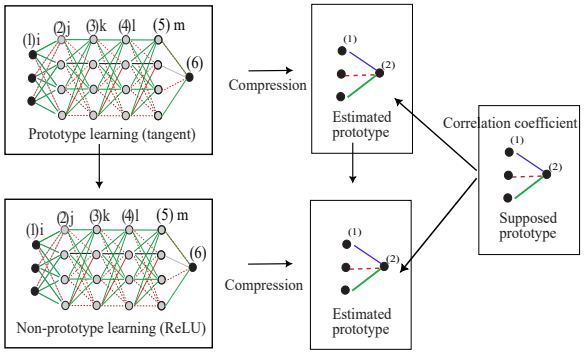

Figure 2: Concept of supposed and estimated prototype with prototype and non-prototype learning.

3.3 Prototype Network

We here show how to compute the prototype and measure the similarity between the estimated and supposed prototypes. Figure 2 illustrates the concept of the actual prototype and the supposed prototype. The supposed prototype is composed of connection weights, calculated as the normalized correlation coefficients between inputs and outputs. This weight configuration does not aim to faithfully represent the relationships between inputs and outputs but rather to represent those relationships as minimally as possible.

The actual prototype can be obtained by compressing the original network. In the figure, a multi-layered neural network with a hyperbolic tangent activation function is trained and compressed into an estimated prototype. In the later stage of learning, we use the ReLU activation function. The multi-layered neural network with the ReLU activation function is then compressed into another prototype. These estimated prototypes are compared with the supposed one.

In evaluating the learning processes, we use potentiality and ratio potentiality. Potentiality represents the degree of organization of connection weights and is akin to conventional entropy, while ratio potentiality measures the similarity between estimated and supposed prototypes. Specifically, ratio potentiality aims to identify which input is more important than others in terms of the strength of connection weights. Thus, it is not necessary to estimate the similarity of actual connection weights, but rather the similarity of individual potentiality. For the computation of entropy, divergence, and compression from multi-layered neural networks to the prototypes, see Appendix.

The potentiality of a neural network is based on

the strength of connection weights. This simplification helps clarify the properties of the prototype. Here, we show how to compute potentiality only for a prototype network configuration, i.e., a network without hidden layers, as shown in Figure 2. The individual potentiality or absolute connection weight for the estimated prototype is given by:

$$u_i = \mid w_i \mid, \tag{3}$$

where w denotes the connection weights from the ith neuron to the output neuron. For simplicity, we assume that all individual potentialities are greater than zero. Then, the relative individual potentiality is computed for the estimated and compressed prototype, labeled (1,6):

$$g_i^{(1,6)} = \frac{u_i^{(1,6)}}{\max_{i'} u_{i'}^{(1,6)}}. \tag{4}$$

Next, the potentiality is computed by summing all individual ones:

$$G = \sum_i g_i^{(1,6)}. \tag{5}$$

The potentiality is bounded and can be normalized for easier interpretation in the explanation of experimental results. Additionally, we compute the relative individual potentiality for the supposed prototype:

$$z_i^{(1,2)} = \frac{c_i^{(1,2)}}{\max_{i'} c_{i'}^{(1,2)}}, \tag{6}$$

where c denotes the individual potentiality, namely the correlation coefficients between inputs and the target in the training data set. We can also compute the potentiality for the supposed prototype:

$$Z = \sum_i z_i^{(1,2)}. \tag{7}$$

The potentiality is similar to the entropy function, and it is developed to simplify the computation of entropy. As with entropy, when all the relative potentialities are the same, the potentiality reaches its maximum. On the other hand, if only one potentiality is larger than any of the others, the potentiality becomes smaller.

In addition to this standard potentiality, we introduce the ratio potentiality for comparison between the estimated and supposed prototypes. The ratio of compressed individual potentiality to supposed individual potentiality can be computed by:

$$r_i^{(1,6)} = \frac{g_i^{(1,6)}}{z_i^{(1,2)}}. \tag{8}$$

For this ratio r_i, we compute the ratio potentiality:

$$R^{(1,6)} = \sum_i \frac{r_i^{(1,6)}}{\max_{i'} r_{i'}^{(1,6)}}. \tag{9}$$

When all the ratio potentialities are equal, the ratio potentiality becomes larger. On the other hand, if only one ratio potentiality is larger than the others, the ratio potentiality becomes smaller. We should note here that ratio potentiality is introduced primarily to detect which input is more important than others in terms of the corresponding potentialities. When used as a measure of similarity, the corresponding connection weights should be carefully examined for actual interpretation.

4 RESULTS AND DISCUSSION

4.1 Experimental Outline

The preliminary experiments used the bankruptcy data (Shimizu, 2009). In this section, first, we explain the experimental results using the tangent and ReLU activation functions separately. The results confirmed that the tangent activation function could more explicitly extract the prototype network than the ReLU function. Then, by combining the tangent and ReLU functions, we demonstrate how this combination could be used to improve generalization. Finally, by examining individual connection weights as well as the corresponding ratio potentialities, we show how the combination of the two functions could extract both prototype and non-prototype features.

The data was composed of 1,040 input patterns and six input variables, augmented from the original 130 inputs. The data augmentation was only for stabilizing our final results. Without this data augmentation, we could achieve similar results with some instability in the final outcomes. To facilitate easy reproduction of these results, we used the Pytorch neural network package with default parameter values, except for the activation function (hyperbolic tangent and ReLU). These default parameters and standard activation functions were used to ensure that the present results could be reproduced as easily as possible. Finally, all the values were averaged over ten runs and normalized for easy interpretation.

Before delving into the details, we should summarize the main results as follows:

- The networks with the tangent activation function could clearly detect the prototype at the very beginning of learning in Figure 3. On the other hand,

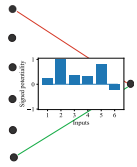

Figure 3: The actual prototype with signed individual potentialities (weights). The weights were actually normalized correlation coefficients between inputs and targets in the training data set.

the ReLU activation function detected the prototype less clearly than the tangent activation function. This can be explained by the loss of information on negative weights that occurred during learning with the ReLU activation function.

- By combining the tangent and ReLU activation functions in one framework, generalization could be improved to an almost maximum level. This demonstrates the utility of combining prototype learning with non-prototype learning, which is ideally supposed to exist behind any learning in neural networks. Though our method did not aim to improve generalization, we reported better generalization results because many methods similar to our present method in multiple activation learning strive hard to improve generalization performance.
- Because the non-prototype learning of the ReLU activation was naturally influenced by the prototype learning with the tangent activation function, the final connection weights tended to be similar to those of the prototype obtained at the beginning. This means that even though improved generalization performance could be achieved by considering detailed information of inputs in the non-prototype learning with the ReLU activation function, the final internal representation was based on the prototype, making interpretation much easier.

4.2 Single and Independent Activation Learning

We used two different activation functions to improve generalization performance, namely, the hyperbolic tangent and ReLU activation functions. The experiment confirmed that the hyperbolic tangent function showed better generalization performance. On the other hand, the ReLU activation function produced lower generalization performance. This is because the potentiality decreased more rapidly than it did with the hyperbolic tangent activation function. A decrease in potentiality means that the number of effective connection weights decreases.

Figure 4 shows the potentiality (left), divergence (middle), and generalization accuracy (right) of networks with no hidden layers (a), with ten hidden layers and the hyperbolic tangent activation function (b), and the ReLU activation function (c). As shown in Figure 4(a), without hidden layers, the accuracy (right) increased very gradually and could not reach a high level of generalization. The potentiality (left) and divergence (middle) increased and then decreased, indicating that connection weights were not well-organized for improved generalization. When the hyperbolic tangent activation function was used, as shown in Figure 4(b), the potentiality decreased slowly and consistently, while the divergence (middle) remained unchanged. Since the generalization (right) showed higher values in the end, the decrease in potentiality, corresponding to the organization of connection weights, is one of the main reasons for this improvement. Figure 4(c) shows the results of using the ReLU activation function. The potentiality decreased more rapidly than with the hyperbolic tangent activation function, indicating that connection weights were more organized than with the hyperbolic tangent activation. The divergence (middle) decreased slightly but remained almost unchanged throughout the entire learning process. The generalization accuracy (right) was slightly lower than that of the hyperbolic tangent activation function.

The results show that the hyperbolic tangent activation function could improve generalization better than the ReLU activation function. This is due to the more rapid decrease in potentiality and the correspondingly overly organized connection weights produced by the ReLU function in terms of the number of connection weights.

For the ratio potentiality, the hyperbolic tangent function could detect it immediately at the beginning, but the ReLU activation function failed to do so. Figure 5 shows the ratio (left), divergence (middle), and correlation coefficients between estimated and supposed prototypes (right). One of the main results is that the ratio potentiality (left) of the hyperbolic tangent activation function produced much higher values at the very beginning, as shown in Figure 5(b). In fact, the highest value was 0.841, close to the maximum value, and it was achieved in only 73 steps, as shown in Table 1. The correlation coefficient (right) also produced higher values at the beginning, but they were not as explicit as the ratio potentiality. The divergence (middle) did not show the lowest and optimal values at the beginning. On the other hand, the networks without hidden layers in Figure 5(a) and those with

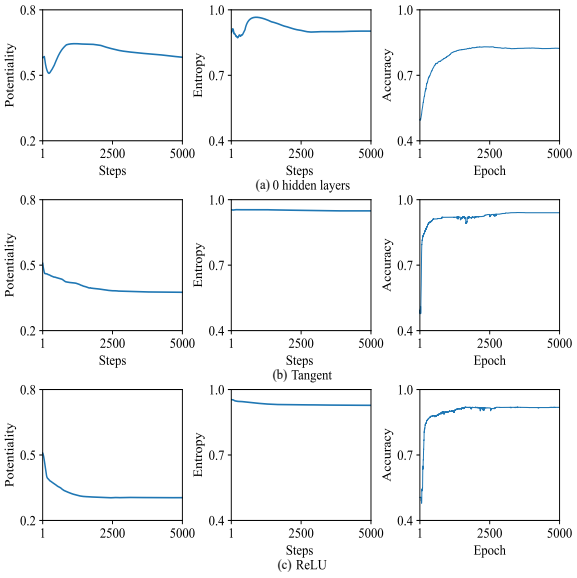

Figure 4: Potentiality (left), entropy (middle) and generalization accuracy (right) as a function of the number of learning steps (epochs) by networks with no hidden layers (a), 10 hidden layers with the hyperbolic tangent function (b), with the ReLU function (c).

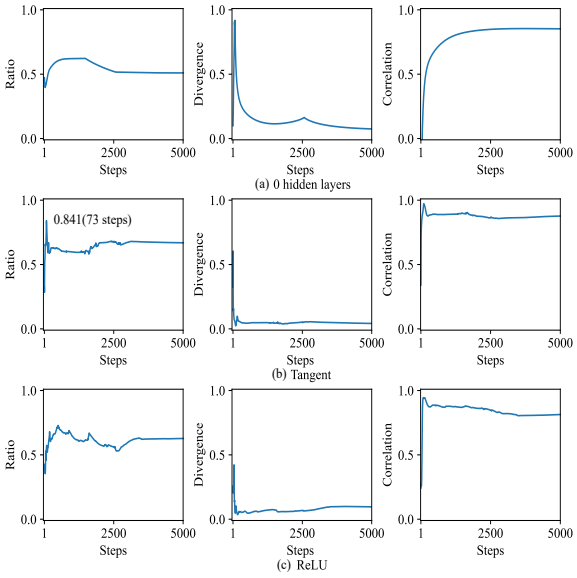

Figure 5: Ratio potentiality (left), divergence (middle) and correlation coefficient (right) as a function of the number of learning steps (epochs) by networks with no hidden layers (a), 10 hidden layers with the tangent hyperbolic function (b), with the ReLU function (c).

the ReLU activation function in Figure 5(c) showed higher values for the ratio potentiality and lower values for the divergence at the beginning, but they were not as explicit as those produced by the hyperbolic tangent activation function. The correlation coefficients (right) showed higher values at the beginning, but they were less clear than those produced by the hyperbolic tangent activation function. This means that the hyperbolic tangent activation function with multi-layered neural networks could clearly detect the prototype in terms of ratio potentiality.

4.3 Prototype and Prototype Learning

By using multiple activations with the hyperbolic tangent and ReLU activation functions, the properties of the tangent activation function seemed to be preserved during learning with the ReLU activation function. This combination effect should result in better generalization and, in particular, easier interpretation.

Figure 6 shows the results of using multiple activations with the hyperbolic tangent and ReLU activation functions when the number of prototype learning steps increased from 500 (a) to 1500 (c). The potentiality on the left decreased naturally, similar to that of the hyperbolic tangent function, as shown in Figure 6(b). However, the entropy remained unchanged and was not effective in describing the learning and organization processes. The generalization performance on the right shows a rapid increase when the activation function was switched to the ReLU function after a sharp decline in generalization. In particular, when the number of learning steps for the prototype learning with the tangent activation function was 1000, as shown in Figure 6(b), the generalization accuracy was close to the maximum value.

Figure 7 shows the ratio (left), divergence (middle), and correlation coefficients (right) when the number of learning steps increased from 500 (a) to 1500 (c). Naturally, at the beginning, higher ratio potentiality and correlation coefficient values were observed due to the tangent activation function. When the activation function was switched to the ReLU activation function, the ratio and, less clearly, the correlation coefficient became slightly higher, while the divergence remained small. The ratio potentiality tended to increase when the activation was switched to the ReLU function. In particular, when the number of learning steps for prototype learning was 500, as shown in Figure 7(a), the increase in ratio potentiality was more explicitly observed. This is expected, as the effect of higher ratio potentiality persisted at the beginning of learning. The ratio potentiality clearly detected the effect of prototype learning at the beginning, while the divergence and correlation coefficient detected this effect less clearly.

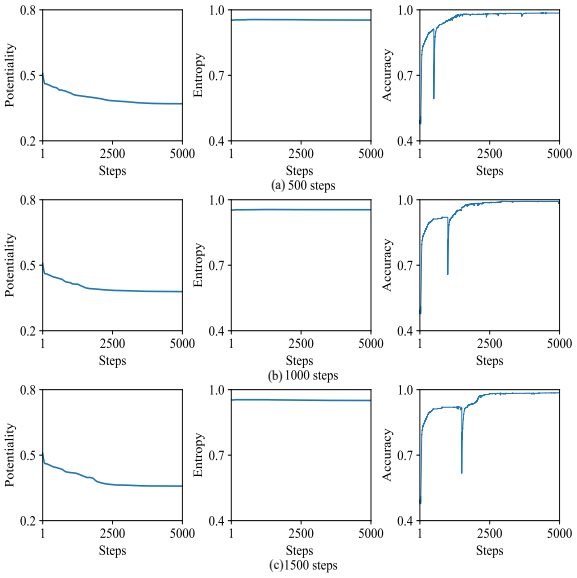

Figure 6: Potentiality (left), entropy (middle) and generalization accuracy (right) as a function of the number of learning steps (epochs) by the multi-activation with 500 (d), 1000 (e) and 1500 (f) learning steps for the first learning steps with the hyperbolic tangent and the remaining ones with the ReLU function.

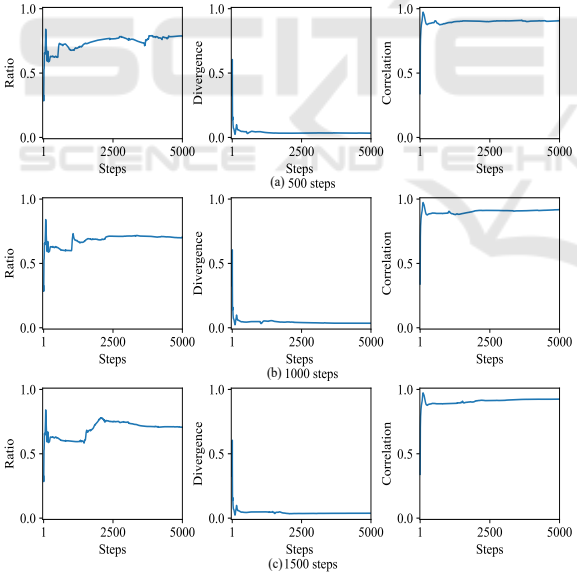

Figure 7: Ratio potentiality (left), divergence (middle) and correlation coefficient (right) as a function of the number of learning steps (epochs) by the multiple activations with 500 (d), 1000 (e) and 1500 (f) learning steps for the first learning steps with the hyperbolic tangent and the remaining ones with the ReLU function.

4.4 Individual Potentialities

The hyperbolic tangent activation function could detect the prototype around the 100th learning step. At this point, input No.5 was detected as important in a linear manner, while input No.1 was detected as important in a non-linear manner.

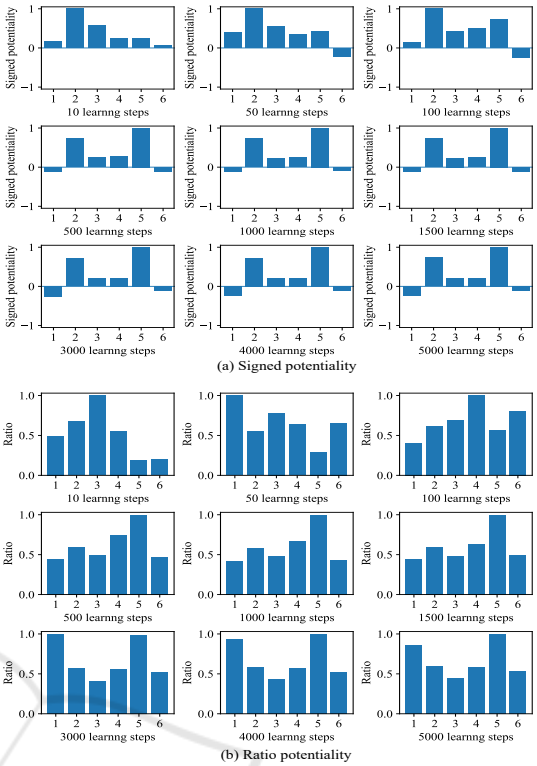

Figure 8: Signed ratio potentialities when the tangent fiction was used with the best generalization in the single activation.

Figure 8(a) shows the signed individual potentialities or connection weights when the number of learning steps increased from 10 to 5000 using only the hyperbolic tangent activation function. As can be seen in the figure, the potentialities became most similar to the prototype shown in Figure 3 around the 100th learning step, where input No.2 had the largest potentiality. Gradually, input No.5 surpassed input No.2 in potentiality. Figure 8(b) shows the individual ratio potentialities as the number of learning steps increased from 10 to 5000. Over time, input No.5, as well as input No. 1, became more significant than the other inputs. Input No.5 had a higher correlation coefficient in the prototype, while input No.1 had a lower correlation coefficient. This indicates that the hyperbolic tangent activation function initially detected linear correlations most strongly, and later also identified non-linear correlations for input No.1 as important.

The ReLU activation function produced outputs based on inputs No.4 and No.6, which were not considered important in the supposed prototype. Figure 9(a) shows the signed individual potentialities or con-

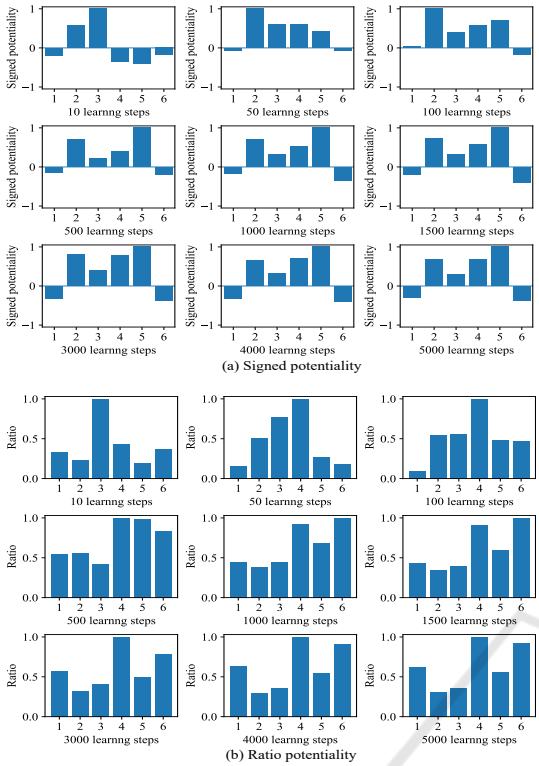

Figure 9: Signed ratio potentialities when the ReLU function was used in the single activation.

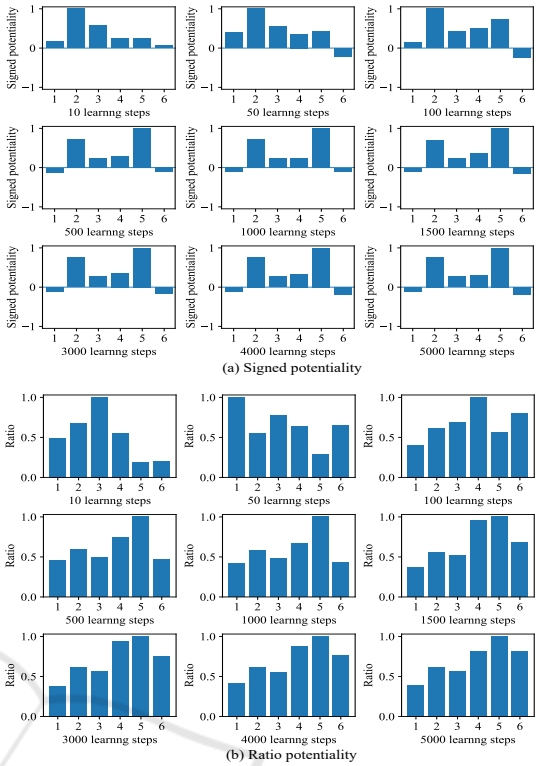

Figure 10: Signed ratio potentialities when the tangent (1000 steps) and ReLU fuction were used with the best generalization.

nection weights with the ReLU activation function. The potentialities became relatively similar to the supposed prototype around the 100th learning step, but the similarity was not very high. Gradually, input No.5 became more prominent in the learning process. Figure 9(b) shows the individual ratio potentialities. One important point to note is that inputs No.4 and No.6 had larger values by the end of the learning process. However, these inputs did not have large weights or correlation coefficients in the prototype, indicating that they were not strongly linearly connected to the outputs. This suggests that the ReLU activation function learned the input patterns in a non-linear manner.

The results from the multiple activations show that combining two different activation functions allows for the simultaneous use of linear and non-linear relations, improving generalization while retaining the simple properties of the prototype for easier interpretation. Figure 10(a) shows the results of signed individual potentialities or connection weights from multiple activation learning using tangent and ReLU activation functions, achieving the best generalization. Because the tangent activation function was used for the first 1000 learning steps, the signed potentialities became naturally similar to those from the hyperbolic tangent activation function. Moreover, in the remaining learning steps, the individual potentialities were close to those from the tangent activation function in Figure 8.

Figure 10(b) shows the ratio potentialities when multiple activation learning was used. Using the ratio potentiality, different results were obtained. For example, one key characteristic is that the ratio potentiality increased with the input number. In particular, the final three inputs, namely inputs No.4 to No.6, had larger potentialities. As explained in Figure 9, inputs No.4 and No.6 had larger potentialities with the single ReLU activation function. On the other hand, input No.5 had relatively larger potentiality in the prototype, as shown in Figure 3. This indicates that multiple activation learning aimed to strengthen both linear and non-linear relations between inputs and outputs.

The results demonstrate that the tangent activation function strongly detected linear and non-linear relations, while the ReLU function focused on non-linear ones. By combining them in multi-activation, both linear and non-linear relations could be detected. This multiple activation learning approach improved generalization more effectively, with prototype learning by the tangent activation function and non-prototype

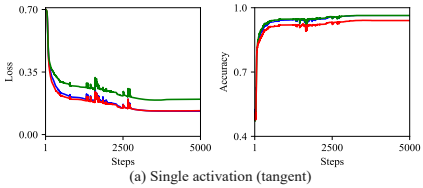

(a) Single activation (tangent)

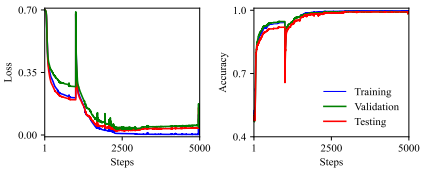

(b) Multiple activations (tangent+ReLU)

Figure 11: Loss (error) and accuracy by the single activation (tangent) and multiple activation learning (tangent+ReLU).

learning by the ReLU function contributing to the enhanced generalization. Additionally, because the final connection weights retain the characteristics of the supposed prototype from the prototype learning, it is much easier to understand the inner workings of the neural network. The estimated idealized prototype learning, achieved by combining the tangent and ReLU activation functions, clearly demonstrates the existence and utility of the concept of idealized prototype learning for interpreting multi-layered neural networks.

4.5 Smaller Variation of Generalization

The reason why better generalization was achieved can be explained by examining the error (loss) and accuracy values computed over ten different runs. This indicates that multiple activation learning can reduce variations in accuracy.

Figure 11 shows the error (left) and accuracy (right) for single activation and multiple activation learning, with the number of steps for prototype learning set to 1000 for optimal generalization performance. As seen in Figure 11(a), when only the hyperbolic tangent activation function was used, discrepancies between validation (green) and testing values (red) increased from the beginning. In contrast, when multiple activation learning was employed in Figure 11(b), the discrepancy decreased immediately after introducing the non-prototype learning with the ReLU activation function, following the sharp decline associated with the change in activation function. This reduction in the variation of generalization errors and accuracies is clearly related to the improved generalization.

Table 1: Summary of experimental results on average ratio, divergency, correlation, and generalization accuracy by networks without hidden layers, tangent, ReLU activation function and three types of multiple activations(changing the number of steps in the prototype learning from 500 to 1500). Bold type letters indicate optimal values. The upper and lower number represent the actual values and the corresponding number of learning steps.

Activ	Ratio	Diverg	Correl	General
	0.624	0.074	0.855	0.824
	1460	5000	3710	4901
Tangent	**0.841**	**0.024**	**0.973**	0.941
	73	96	103	3470
ReLU	0.729	0.035	0.945	0.917
	492	165	87	4185
500	**0.841**	**0.024**	**0.973**	0.985
	73	96	103	4514
1000	**0.841**	**0.024**	**0.973**	**0.992**
	73	96	103	3047
1500	**0.841**	**0.024**	**0.973**	0.984
	73	96	103	4253

4.6 Numerical Summary

Numerical results show that detecting the prototype at the beginning of learning can contribute to improved generalization. This implies that ideal learning with both prototype and non-prototype components can enhance generalization. Additionally, non-prototype learning is performed while maintaining the trace of prototype learning. The interpretation of the inner mechanism is much easier because the prototype represents the simplest network within the given network resources.

Table 1 summarizes the numerical analysis. The network without hidden layers produced the lowest ratio potentiality (0.624), the largest divergence (0.074), the lowest correlation coefficient (0.855), and the lowest generalization (0.824). This indicates that without hidden layers, it is difficult to disentangle the relations between inputs and outputs, making it difficult to extract the prototype. The tangent activation function produced the highest ratio potentiality (0.841) and the highest correlation coefficient (0.973), along with the smallest divergence (0.024), except for the generalization performance (0.941). The ReLU activation function resulted in the second lowest ratio potentiality (0.729), the second lowest correlation coefficient (0.945), and the second highest divergence (0.035). Additionally, the generalization (0.917) was the second lowest. When multiple activation learning was introduced, the ratio potentiality, divergence, and correlation coefficient were similar to those obtained with the tangent activation function. However, the

generalization performance reached the highest value (0.992) when the number of learning steps in prototype learning was 1000. Even in other multiple activation learning cases, generalization (0.984 and 0.985) was significantly better than that of the single activation models (0.941 and 0.917).

The results confirm that detecting and combining prototype and non-prototype learning can contribute to improved generalization and interpretation. In particular, interpretation is greatly facilitated because the prototype, with its minimal network configuration, has a considerable effect on learning.

5 CONCLUSION

The present paper aimed to demonstrate that neural learning should begin with the extraction of the prototype, the simplest network within the given network resources, followed by non-prototype learning on detailed input information. The prototype is intended to be determined as independently as possible from any inputs, though ideally. The importance of the prototype can be demonstrated by comparing a network that easily acquires the prototype with one that does not, using multi-activation techniques. By changing the activation function from the hyperbolic tangent at the beginning to the ReLU function in later learning steps, we observed a significant improvement in generalization performance. Additionally, the final weights retain the trace of the prototype learning from the beginning and are easily understood. The extraction of the prototype should play a critical role in training neural networks, making their internal representations more comprehensible and enhancing generalization.

Finally, we should address several future directions. First, we need to resolve issues inherent to potentiality and ratio potentiality. Due to its simplicity and stability, potentiality is limited to the absolute values of connection weights. The ratio potentiality attempts to estimate how much the estimated individual potentiality exceeds the supposed potentiality. This simplification is used to highlight the importance of inputs for easier interpretation, as larger weights are considered more important. However, in actual scenarios discussed in this paper, negative weights appear to play significant roles in some cases. Thus, it is necessary to incorporate the negative effect or "negative potentiality" to make the potentiality framework more general. Second, exploring different types of activation functions for prototype extraction is possible. In the multiple activation learning, only two standard activation functions were used for ease of reproduction, but many other activation functions exist. It would be interesting to use them for extracting the ideal prototype. Additionally, it may be possible to identify a single activation function or an idealized activation function that captures the properties of both prototype and non-prototype learning. Finally, applying the method to larger and more practical datasets is crucial to determine if our approach can address practical problems that require not only improved generalization but also enhanced interpretation. Understanding the inner workings of neural networks is considered more important than merely improving generalization.

REFERENCES

Apicella, A., Donnarumma, F., Isgrò, F., and Prevete, R. (2021). A survey on modern trainable activation functions. *Neural Networks*, 138:14–32.

Buciluǎ, C., Caruana, R., and Niculescu-Mizil, A. (2006). Model compression. In *Proceedings of the 12th ACM SIGKDD international conference on Knowledge discovery and data mining*, pages 535–541. ACM.

Carlucci, L. and Case, J. (2013). On the necessity of u-shaped learning. *Topics in cognitive Science*, 5(1):56–88.

Case, J. and Kötzing, T. (2016). Strongly non-u-shaped language learning results by general techniques. *Information and Computation*, 251:1–15.

Chao, W.-L., Changpinyo, S., Gong, B., and Sha, F. (2016). An empirical study and analysis of generalized zero-shot learning for object recognition in the wild. In *Computer Vision–ECCV 2016: 14th European Conference, Amsterdam, The Netherlands, October 11-14, 2016, Proceedings, Part II 14*, pages 52–68. Springer.

Corkery, M., Matusevych, Y., and Goldwater, S. (2019). Are we there yet? encoder-decoder neural networks as cognitive models of english past tense inflection. *arXiv preprint arXiv:1906.01280*.

Emanuel, R. H., Docherty, P. D., Lunt, H., and Möller, K. (2024). The effect of activation functions on accuracy, convergence speed, and misclassification confidence in cnn text classification: a comprehensive exploration. *The Journal of Supercomputing*, 80(1):292–312.

Jagtap, A. D. and Karniadakis, G. E. (2023). How important are activation functions in regression and classification? a survey, performance comparison, and future directions. *Journal of Machine Learning for Modeling and Computing*, 4(1).

Kim, J., Oh, T.-H., Lee, S., Pan, F., and Kweon, I. S. (2019). Variational prototyping-encoder: One-shot learning with prototypical images. In *Proceedings of the IEEE/CVF Conference on Computer Vision and Pattern Recognition*, pages 9462–9470.

Kirov, C. and Cotterell, R. (2018). Recurrent neural networks in linguistic theory: Revisiting pinker and

prince (1988) and the past tense debate. *Transactions of the Association for Computational Linguistics*, 6:651–665.

Neill, J. O. (2020). An overview of neural network compression. *arXiv preprint arXiv:2006.03669*.

Nwankpa, C., Ijomah, W., Gachagan, A., and Marshall, S. (2018). Activation functions: Comparison of trends in practice and research for deep learning. *arXiv preprint arXiv:1811.03378*.

Pinker, S. and Prince, A. (1988). On language and connectionism: Analysis of a parallel distributed processing model of language acquisition. *Cognition*, 28(1-2):73–193.

Pourpanah, F., Abdar, M., Luo, Y., Zhou, X., Wang, R., Lim, C. P., Wang, X.-Z., and Wu, Q. J. (2022). A review of generalized zero-shot learning methods. *IEEE transactions on pattern analysis and machine intelligence*, 45(4):4051–4070.

Ramachandran, P., Zoph, B., and Le, Q. V. (2017). Searching for activation functions. *arXiv preprint arXiv:1710.05941*.

Rumelhart, D. E. and McClelland, J. L. (1986). On learning the past tenses of English verbs. In Rumelhart, D. E., Hinton, G. E., and Williams, R. J., editors, *Parallel Distributed Processing*, volume 2, pages 216–271. MIT Press, Cambrige.

Saralajew, S., Holdijk, L., Rees, M., and Villmann, T. (2018). Prototype-based neural network layers: incorporating vector quantization. *arXiv preprint arXiv:1812.01214*.

Shimizu, K. (2009). *Multivariate analysis (in Japanese)*. Nikkan Kogyo Shinbun.

Song, Y., Wang, T., Cai, P., Mondal, S. K., and Sahoo, J. P. (2023). A comprehensive survey of few-shot learning: Evolution, applications, challenges, and opportunities. *ACM Computing Surveys*, 55(13s):1–40.

Sütfeld, L. R., Brieger, F., Finger, H., Füllhase, S., and Pipa, G. (2020). Adaptive blending units: Trainable activation functions for deep neural networks. In *Intelligent Computing: Proceedings of the 2020 Computing Conference, Volume 3*, pages 37–50. Springer.

Viering, T. and Loog, M. (2022). The shape of learning curves: a review. *IEEE Transactions on Pattern Analysis and Machine Intelligence*.

Westermann, G. (2022). Emergent modularity and u-shaped learning in a constructivist neural network learning the english past tense. In *Proceedings of the Twentieth Annual Conference of the Cognitive Science Society*, pages 1130–1135. Routledge.

APPENDIX

Entropy and Divergence

As mentioned above, potentiality is computed to simplify entropy and its corresponding divergence. We introduce the entropy and its related divergence measure here. The relative potentiality for the supposed prototype network is computed by

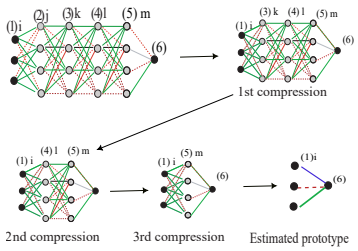

Figure 12: Concept of compression prototype.

$$q_i^{(1,2)} = \frac{c_i^{(1,2)}}{\sum_{i'} c_{i'}^{(1,2)}}. \tag{10}$$

Next, the relative potentiality for the compressed and estimated prototype network is computed by

$$p_i^{(1,6)} = \frac{u_i^{(1,6)}}{\sum_{i'} u_{i'}^{(1,6)}}. \tag{11}$$

Entropy can be defined by

$$H^{(1,6)} = -\sum_i p_i^{(1,6)} \log p_i^{(1,6)}. \tag{12}$$

Divergence, being the reverse type, is computed by

$$D^{(1,6)} = \sum_i p_i^{(1,6)} \log \frac{p_i^{(1,6)}}{q_i^{(1,2)}}. \tag{13}$$

This divergence decreases when the potentialities of the two networks become more similar to each other.

Compression

In the first compression, the weights from the input layer to the third layer, labeled (1,3), are compressed as follows:

$$w_{ik}^{(1,3)} = \sum_j w_{ij}^{(1,2)} w_{jk}^{(2,3)}. \tag{14}$$

By repeating these processes, we obtain the compressed weights connecting the first and fifth layers, denoted as $w_{iq}^{(1,5)}$. Using these connection weights, we finally obtain the fully compressed weights for (1,6):

$$w_i^{(1,6)} = \sum_q w_{iq}^{(1,5)} w_q^{(5,6)}. \tag{15}$$

In the context of large multi-layered neural networks, there are many different types of compression methods. This compression method differs from

conventional and popular compression methods (Buciluǎ et al., 2006; Neill, 2020). The majority of these conventional methods attempt to compress the original multi-layered neural networks without considering internal configurations, focusing instead on generalization performance. This paper aims to understand the inner workings of neural networks, and thus it is necessary to preserve the internal configurations of the original multi-layered neural networks as much as possible.